

Terahertz Wireless Transmissions with Maximal Ratio Combining over Fluctuating Two-Ray Fading

Atharva Anand Joshi, Pranay Bhardwaj, and S. M. Zafaruddin

Department of Electrical and Electronics Engineering, BITS Pilani, Pilani Campus, Pilani-333031, Rajasthan, India
Email: {f20180515, p20200026, syed.zafaruddin}@pilani.bits-pilani.ac.in

Abstract—Mitigating channel fading and transceiver impairments are desirable for high-speed terahertz (THz) wireless links. This paper analyzes the performance of a multi-antenna THz wireless system by considering the combined effect of pointing errors and fluctuating two-ray (FTR) fading model. We provide a statistical characterization of the maximal ratio combining (MRC) receiver over independent and nonidentical (i.n.i.d.) channel conditions in terms of multi-variate Fox's H by deriving density and distribution functions of the signal-to-noise ratio (SNR) of a single-link THz link using incomplete Gamma function. We develop exact analytical expressions of outage probability, average bit-error-rate (BER), and ergodic capacity for both single-antenna and MRC receivers. We also present the diversity order of the system by deriving asymptotic expressions for outage probability and average BER at high SNR to obtain insights into the system performance. We validate our derived analytical expressions with Monte-Carlo simulations and demonstrate the effect of various system and channel parameters on the performance of single and multi-antenna THz wireless communications.

Index Terms—Beyond 5G/6G wireless systems, fluctuating two ray, performance analysis, pointing error, maximal ratio combining, probability distribution function, terahertz communication.

I. INTRODUCTION

Terahertz (THz) wireless is an upcoming technology to provide new spectrum resources for future communication systems. The availability of contiguous high bandwidth transmissions in the THz spectrum can be potential for wireless backhaul/fronthaul technology [1]–[3]. The THz spectrum is mostly unlicensed and can support secured terabits per second (Tbps) data transmissions with low latency for various high-end applications. The line-of-sight (LOS) THz technology requires high directional antennas with higher gain to compensate for severe path loss due to the molecular absorption of transmitted signals. Nevertheless, the THz link is susceptible to the random pointing errors caused by the misalignment between transmitter and receiver antenna beams and may incur transceiver distortion at higher frequencies in addition to the stochastic multi-path fading [4]–[7]. Alleviating the adverse effects of signal attenuation and fading is desirable for high-speed THz links.

Recently, dual-hop and multi-hop relaying at THz frequencies have been investigated [8]–[16]. More specifically, the authors in [8] formulated an optimal relaying distance for THz-band communication to maximize the network throughput.

This work was supported in part by the Start-up Research Grant, Department of Science Technology (DST), Science and Engineering Research Board (SERB), India under Start-up Research Grant SRG/2019/002345.

In [9], a relay selection approach was suggested to mitigate the impact of antenna misalignment and shadowing due to the human blockage in a multi-relay setup. A reconfigurable intelligent surface (RIS) assisted multi-hop THz system over Rician fading was considered in [11] to mitigate the signal attenuation using deep reinforcement learning (DRL) based beam-forming technique. Considering the generalized α - μ fading combined with stochastic pointing errors, the decode-and-forward (DF) protocol was employed to link THz and radio frequency (RF) technologies [12], [13]. Using multi-antenna transceivers, the DF relaying was studied for a dual-hop THz-THz link [10].

There has been an increased research interest to model the short-term fading for THz communications [17]–[20]. A Gamma mixture channel model for THz transmissions for a short (< 1 m) link is proposed in [18]. The authors in [19] find α - μ fading model suitable for the THz transmission using the measurement at 152GHz for a link length within 50m. Using a comprehensive THz measurement data at 300GHz for train-to-infrastructure and inside station [21], the authors in [20] demonstrate that the fluctuating two ray (FTR) model is a better fit for THz multi-path fading modeling than the conventional Rician and Nakagami-m distributions. Using the combined effect of the short-term FTR fading, antenna misalignment, and hardware impairments, [20] derived outage probability and ergodic capacity for RIS-aided THz systems.

The recently proposed FTR model has been extensively studied for mmWave wireless transmissions [22]–[27]. In [22]–[24], analytical performance was studied for a single-link FTR fading channel. The physical layer secrecy performance over the FTR fading channel was analyzed [25]. The authors in [26] analyzed the performance of a mixed free-space-optics (FSO)-mmWave system by modeling the mmWave and FSO channels as FTR and Gamma-Gamma distributed, respectively. In contrast to the single-antenna system, multi-antenna at the receiver can harness the spatial diversity over independent fading for improved performance [28]–[32]. In [28], the authors analyzed the performance of an equal gain combining (EGC) receiver by deriving outage probability and average BER using single-variate mathematical functions over FTR fading channels. In [29], a low complexity selection combining receiver was investigated with a performance analysis on the outage probability, average BER, and ergodic capacity in terms of multi-variate Fox's H function. In [30], the authors analyzed the optimal maximal ratio combining (MRC) receiver by deriving the PDF and CDF of the sum of arbitrarily distributed FTR variates. In [31], the outage probability and an upper

bound on average BER was derived for the MRC receiver. The authors in [32] provided asymptotic and non-asymptotic expressions of the outage probability and average BER for the MRC over non-identical distributed FTR fading channels. The moment matching method was used to approximate statistics of the sum of FTR fading channel for analyzing relay-assisted radio frequency (RF)-mmWave wireless communications for high-speed trains [33].

In the light of THE above research and to the best of the author's knowledge, performance analysis of the MRC receiver with THz wireless transmissions over FTR fading channels jointly with stochastic pointing errors is not available in the open literature. Our main contributions of this paper are follows:

- By deriving PDF and CDF of a single-link THz link using standard mathematical functions, we provide exact statistical characterization of the SNR for the MRC receiver under the joint effect of FTR short-term fading and zero-bore sight pointing errors considering independent and nonidentical (i.n.i.d.) channel conditions in terms of multi-variate Fox's H function.
- We develop exact analytical expressions of ergodic capacity, outage probability, and average BER for both single-antenna reception and MRC receiver and present asymptotic expressions for outage probability and average BER at high SNR. We derive the diversity order of the considered system to show the advantage of multi-antenna reception and the impact of pointing errors.
- We evaluate multi-variate Fox's H function using Python code [34] and validate our derived analytical expressions with Monte-Carlo simulations. We also demonstrate the effect of various system and channel parameters on the performance of THz wireless communications.

II. SYSTEM MODEL

A single-antenna source communicates to an L -antenna destination over the THz spectrum. The THz link is affected by path-loss, short-term fading, pointing errors, and transceiver distortions. Assuming negligible hardware impairments [12], [35], the received signal y_i at the i -th antenna is given by:

$$y_i = h_l h_i s + w_i, \quad (1)$$

where h_l is the path gain, s is the transmitted signal with power P , h_i denotes the fading channel coefficient, and w_i is the additive white Gaussian noise with a variance σ_w^2 . The deterministic path gain h_l is dependent on antenna gains, frequency, and molecular absorption coefficient [6]:

$$h_l = \frac{c\sqrt{G_t G_r}}{4\pi f d} \exp\left(-\frac{1}{2}k(f)d\right) \quad (2)$$

where c , f , and d respectively denote the speed of light, carrier frequency, link distance whereas G_t and G_r denote gain of the transmitting antenna and receiving antenna, respectively. The term $k(f, T, \psi, p)$ is the molecular absorption coefficient depends on the temperature T , relative humidity ψ , and atmospheric pressure p [36].

The compound channel coefficient is $h_i = h_{pi} h_{fi}$, where h_{pi} and h_{fi} models pointing error and short term fading,

respectively. We use the zero boresight model for pointing errors h_{pi} [37]:

$$f_{h_{pi}}(h_p) = \frac{\phi^2}{S_0 \phi^2} h_p^{\phi^2 - 1}, 0 \leq h_p \leq S_0, \quad (3)$$

where $S_0 = \text{erf}(v)^2$ with $v = \sqrt{\pi/2} (r_1/\omega_z)$ and ω_z is the beam-width, $\phi = \frac{\omega_{zeq}}{2\sigma_s}$ with ω_{zeq} as the equivalent beam-width at the receiver, which is given as $\omega_{zeq}^2 = \omega_z^2 \sqrt{\pi} \text{erf}(v) / (2v \exp(-v^2))$, and σ_s^2 is the variance of pointing errors displacement characterized by the horizontal sway and elevation [37].

To model $|h_{fi}|^2$, we use the FTR fading channel with PDF given as [23]:

$$f_{|h_{fi}|^2}(x) = \frac{m^m}{\Gamma(m)} \sum_{j=0}^{\infty} \frac{K^j d_j x^j}{(\Gamma(j+1))^2 (2\sigma^2)^{j+1}} \exp\left(-\frac{x}{2\sigma^2}\right) \quad (4)$$

where K is the ratio of the average power of the dominant component and multi-path, m is the index of fading severity, and Δ denotes the similarity of two dominant waves. The term σ^2 represents the variance of diffused components such that $\sigma^2 = \frac{1}{2(1+K)}$ for the normalized averaged SNR. The factor d_j is defined in [23] and recently updated with an additional factor in [38].

We denote SNR of the i -th antenna as $\gamma_i = \gamma_0 |h_i|^2$, where $\gamma_0 = \frac{P|h_l|^2}{\sigma_w^2}$. Assuming perfect channel state information (CSI), SNR with optimal combining for the MRC receiver is $\gamma = \sum_{i=1}^L \gamma_i$. Thus, PDF and CDF for the sum of product of pointing errors and FTR random variables is required for statistical performance analysis of the MRC receiver.

III. STATISTICAL DERIVATIONS

In this section, we provide statistical results for the sum of L arbitrarily distributed FTR fading combined with stochastic pointing errors by deriving closed-form expressions of the PDF and CDF of the single THz link.

Proposition 1: If $|h_i| = |h_{fi}| |h_{pi}|$ is the combined effect of FTR fading and pointing errors, then the PDF and CDF of the single-link SNR $\gamma_i = \gamma_0 |h_i|^2$ are given by

$$f_{\gamma_i}(x) = \frac{\phi^2 m^m}{2S_0^{\phi^2} \gamma_0^{\frac{\phi^2}{2}} (2\sigma^2)^{\frac{\phi^2}{2}} \Gamma(m)} \sum_{j=0}^{\infty} \frac{K^j d_j}{[\Gamma(j+1)]^2} x^{\left(\frac{\phi^2}{2}-1\right)} \Gamma\left(-\frac{\phi^2}{2} + j + 1, \frac{x}{2\gamma_0 \sigma^2 S_0^2}\right) \quad (5)$$

$$F_{\gamma_i}(x) = \frac{m^m}{2S_0^{\phi^2} \gamma_0^{\frac{\phi^2+1}{2}} (2\sigma^2)^{\frac{\phi^2}{2}} \Gamma(m)} \sum_{j=0}^{\infty} \frac{K^j d_j}{[\Gamma(j+1)]^2} 2x^{\frac{\phi^2}{2}} \Gamma\left(-\frac{\phi^2}{2} + j + 1, \frac{x}{2\gamma_0 \sigma^2 S_0^2}\right) - 2\phi^{2+1} (\gamma_0 \sigma^2 S_0^2)^{\frac{\phi^2}{2}} x^{-\frac{\phi^2}{2}} \Gamma\left(j + 1, \frac{x}{2\gamma_0 \sigma^2 S_0^2}\right) \quad (6)$$

Proof: Transforming random variable in (3), we get

$$f_{h_{pi}^2}(x) = \frac{1}{2} \phi^2 S_0^{-\phi^2} x^{\frac{\phi^2}{2}-1}, \quad 0 \leq x \leq S_0^2, \quad (7)$$

Using the limits of PDF in (4) and (7), the PDF of $|h_i|^2 =$

$h_{f_i}h_p^2$ can be expressed as [39]

$$f_{h_i^2}(x) = \int_0^{S_0^2} \frac{1}{y} f_{h_{f_i}}\left(\frac{x}{y}\right) f_{h_{p_i}}(y) dy. \quad (8)$$

Substituting (4) and (7) in (8), we have

$$f_{h_i^2}(x) = \sum_{j=0}^{\infty} \frac{K^j d_j}{[\Gamma(j+1)]^2 (2\sigma^2)^{j+1}} x^j \int_0^{S_0^2} e^{-\frac{x}{2y\sigma^2}} y^{\frac{\phi^2}{2}-2-j} dy \quad (9)$$

Expressing the integral in (9) in terms of incomplete Gamma function with a transformation of random variable $\frac{1}{\gamma_0} f_{|h_{f_p}|^2}(\gamma/\gamma_0)$, we get (5). To derive the CDF $F_\gamma(x) = \int_0^x f_\gamma(z) dz$, we use the identity $\int x^{b-1} \Gamma(s, x) dx = -\frac{1}{b} (x^b \Gamma(s, x) + \Gamma(s+b, x))$ to get (6). ■

In the following Theorem, we capitalize the results of Proposition 1 to derive PDF and CDF of the SNR for the MRC receiver:

Theorem 1: If the PDF of single THz link is distributed as (5), then PDF $f_\gamma(\gamma)$ and CDF $F_\gamma(\gamma)$ of the SNR $\gamma = \sum_{i=1}^L \gamma_i$ for an L -antenna MRC receiver are given by

$$f_\gamma(\gamma) = \frac{1}{\gamma} \sum_{[j_i=0]_{i=1}^L} \prod_{l=1}^L \frac{\phi^2 m_l^{m_l}}{2S_0^{\phi^2} \Gamma(m_l)} \frac{K_l^{j_l} d_{l j_l} \gamma^{\phi^2/2}}{[\Gamma(j_l+1)]^2 (2\sigma_l^2 \gamma_0)^{\phi^2/2}} H_{0,1:2,2;2,2;\dots;2,2}^{0,0:2,1;2,1;\dots;2,1} \left[V(\gamma) \left| \begin{matrix} V_1 \\ V_2 \end{matrix} \right. \right] \quad (10)$$

where $V(\gamma) = \left\{ \frac{\gamma}{2\sigma_i^2 S_0^2 \gamma_0} \right\}_{i=1}^L$, $V_1 = - : \{(1 - \frac{\phi^2}{2}, 1), (1, 1)\}; \dots; \{(1 - \frac{\phi^2}{2}, 1), (1, 1)\}$ and $V_2 = \{(1 - \frac{L\phi^2}{2}, 1, \dots, 1)\}; \{(-\frac{\phi^2}{2} + j_i + 1, 1), (0, 1)\}_{i=1}^L$

$$F_\gamma(\gamma) = \sum_{[j_i=0]_{i=1}^L} \prod_{l=1}^L \frac{\phi^2 m_l^{m_l}}{2S_0^{\phi^2} \Gamma(m_l)} \frac{K_l^{j_l} d_{l j_l} \gamma^{\phi^2/2}}{[\Gamma(j_l+1)]^2 (2\sigma_l^2 \gamma_0)^{\phi^2/2}} H_{0,1:2,2;2,2;\dots;2,2}^{0,0:2,1;2,1;\dots;2,1} \left[U(\gamma) \left| \begin{matrix} U_1 \\ U_2 \end{matrix} \right. \right] \quad (11)$$

where $U(\gamma) = \left\{ \frac{\gamma}{2\sigma_i^2 S_0^2 \gamma_0} \right\}_{i=1}^L$, $U_1 = - : \{(1 - \frac{\phi^2}{2}, 1), (1, 1)\}; \dots; \{(1 - \frac{\phi^2}{2}, 1), (1, 1)\}$ and $U_2 = \{(-\frac{L\phi^2}{2}, 1, \dots, 1)\}; \{(-\frac{\phi^2}{2} + j_i + 1, 1), (0, 1)\}_{i=1}^L$

Proof: See Appendix A. ■

IV. PERFORMANCE ANALYSIS

In this section, we analyze the performance of single-antenna THz link in terms of standard Mathematical functions and use multi-variate Fox's H and Gamma functions to provide exact and asymptotic analysis on the multi-antenna reception.

A. Single Antenna Reception (SAR)

1) *Outage Probability:* Outage probability is defined as the probability of instantaneous SNR less than a predetermined threshold value γ_{th} i.e., $P_{out} = P(\gamma < \gamma_{th})$. Thus an exact expression of the outage probability is $P_{out}^{SAR} = F_{\gamma_i}(\gamma_{th})$, where $F_{\gamma_i}(x)$ is given in (6).

2) *Average BER:* Average BER is another important performance metric for communication systems, defined as [40]

$$\bar{P}_e = \frac{q^p}{2\Gamma(p)} \int_0^\infty \exp(-qx) x^{p-1} \Psi_X(x) dx \quad (14)$$

where p and q are constants to specify different modulation techniques and Ψ_X is the CDF. We denote by $\xi = 2\gamma_0\sigma^2 S_0^2$. Using (6) in (14), applying the identity [[41],6.455/1] and expressing the Hypergeometric function into Gamma function we get

$$\bar{P}_e^{SAR} = \frac{m^m p^q}{4S_0^{\phi^2} \gamma_0^{\frac{\phi^2+1}{2}} (2\sigma^2)^{\frac{\phi^2}{2}} \Gamma(m) \Gamma(p)} \sum_{j=0}^{\infty} \frac{K^j d_j}{[\Gamma(j+1)]^2} \times \frac{2(\xi)^{-(\frac{\phi^2}{2}+p)} e^{-q\gamma} \left[-2^{\frac{\phi^2}{2}} (\frac{\phi^2}{2}+p) \Gamma(j+1+p) + p \Gamma(2j+2+p) \right]}{p(\frac{\phi^2}{2}+p)} \quad (15)$$

3) *Ergodic Capacity:* The ergodic capacity is defined as

$$\bar{\eta} = \int_0^\infty \log_2(1+x) \psi_X(x) dx \quad (16)$$

where ψ_X denotes the PDF. Using (5) in (16) and applying identity of definite integration of two Meijer's G function [[42],07.34.21.0011.01], we get an exact expression for the ergodic capacity of the single THz link

$$\bar{\eta}^{SAR} = \frac{m^m}{\log(2) S_0^{\phi^2} \gamma_0^{\frac{\phi^2}{2}} (2\sigma^2)^{\frac{\phi^2}{2}} \Gamma(m)} \sum_{j=0}^{\infty} \frac{K^j d_j}{[\Gamma(j+1)]^2} \xi^{-\frac{\phi^2}{2}} G_{3,4}^{4,1} \left(\begin{matrix} -\frac{\phi^2}{2}, 1 - \frac{\phi^2}{2}, 1 \\ -\frac{\phi^2}{2} + j + 1, 0, -\frac{\phi^2}{2}, -\frac{\phi^2}{2} \end{matrix} \middle| \xi \right) \quad (17)$$

Further, we can use $\log(1+\gamma) > \log(\gamma)$ in (16) with (5), and denoting $\psi^{(0)}$ as the digamma function to get a simpler bound on the ergodic capacity

$$\bar{\eta}^{SAR} \geq \frac{2m^m}{\log(2) \phi^2 S_0^{\phi^2} \gamma_0^{\frac{\phi^2}{2}} (2\sigma^2)^{\frac{\phi^2}{2}}} \Gamma(m) \sum_{j=0}^{\infty} \frac{K^j d_j}{[\Gamma(j+1)]^2} \xi^{\frac{\phi^2}{2}} \Gamma(j+1) \left(-1 - \frac{\phi^2}{2} \log(\xi) + \frac{\phi^2}{2} \psi^{(0)}(j+1) \right) \quad (18)$$

by applying integration-by-parts with the identity [[41], eq.4.352.1].

B. Multi-antenna Reception with MRC

1) *Outage Probability:* An exact expression of the outage probability for the MRC is $P_{out}^{MRC} = F_\gamma(\gamma_{th})$, where $F_\gamma(\gamma)$ is given in (11). We use [43] to present the asymptotic outage probability in (12). Considering the dominant terms at high SNR, we get the diversity order as $\sum_{l=1}^L \min\{j_l + 1, \phi^2/2\}$. It is interesting to note that the diversity order is independent of FTR fading parameters K , m , and Δ as also observed in earlier literature [30], and has been extensively verified for THz transmissions in numerical section V. The diversity order shows the advantage of multi-antenna reception and that the impact of pointing errors can be minimized by circumventing the multi-path fading using a sufficiently higher beam-width.

2) *Average BER:* Substituting $F_\gamma(\gamma)$ in (14) and applying the definition of multivariate Fox's H-function with the following inner integral I_1

$$I_1 = \int_0^\infty e^{-qz} z^{p-1} z^{\sum_{l=1}^L (\frac{\phi^2}{2} + \zeta_l)} dz = \frac{\Gamma\left(p + \frac{L\phi^2}{2} \sum_{l=1}^L \zeta_l\right)}{q^{p + \frac{L\phi^2}{2} + \sum_{l=1}^L \zeta_l}} \quad (19)$$

$$P_{\text{out}}^{\text{MRC},\infty} = \sum_{[j_i=0]_{i=1}^L}^{\infty} \prod_{l=1}^L \frac{\phi^2 m_l^{m_l}}{2A_0^{\phi^2} \Gamma(m_l)} \frac{K_l^{j_l} d_{l j_l} \gamma^{\phi^2/2}}{[\Gamma(j_l+1)]^2 (2\sigma_l^2 \gamma_0)^{\phi^2/2}} \frac{1}{\beta \Gamma\left(\frac{L\phi^2}{2} + \sum_{i=1}^L g_i\right)} \prod_{i=1}^L \frac{\prod_{j=1, j \neq c_i}^2 \Gamma(b_{i,j} + B_{i,j} - B_{i,j} g_i) \Gamma\left(\frac{\phi^2}{2} - 1 + g_i\right)}{\Gamma\left(\frac{\phi^2}{2} - j_i\right)} \left(\frac{\gamma}{2\sigma_i^2 S_0^2 \gamma_0}\right)^{g_i} \quad (12)$$

$$\bar{P}_e^{\text{MRC},\infty} = \frac{1}{2\Gamma(p)q^{\frac{L\phi^2}{2}}} \sum_{[j_i=0]_{i=1}^L}^{\infty} \prod_{l=1}^L \frac{\phi^2 m_l^{m_l}}{2S_0^{\phi^2} \Gamma(m_l)} \frac{K_l^{j_l} d_{l j_l}}{[\Gamma(j_l+1)]^2 (2\sigma_l^2 \gamma_0)^{\phi^2/2}} \frac{\Gamma\left(p + \frac{L\phi^2}{2} + \sum_{i=1}^L g_i\right)}{\beta \Gamma\left(\frac{L\phi^2}{2} + \sum_{i=1}^L g_i\right)} \prod_{i=1}^L \frac{\prod_{j=1, j \neq c_i}^2 \Gamma(b_{i,j} + B_{i,j} - B_{i,j} g_i) \Gamma\left(\frac{\phi^2}{2} - 1 + g_i\right)}{\Gamma\left(\frac{\phi^2}{2} - j_i\right)} \left(\frac{1}{2\sigma_i^2 S_0^2 \gamma_0 q}\right)^{g_i-1} \quad (13)$$

where $b_{i,1} = -\frac{\phi^2}{2} + j + 1$, $b_{i,2} = 0$, $B_{i,1} = 1$, $B_{i,2} = 1$, $g_i = \min\{-\frac{\phi^2}{2} + j_i + 1, 0\}$, $\beta = \prod_{i=1}^L B_{i,c_i}$, and $c_i = \arg \min_{j=1:m_i} \left\{ \frac{b_{i,j}}{B_{i,j}} \right\}$.

and applying the definition of multivariate Fox's H-function on the resultant expression [44], we get

$$\bar{P}_e^{\text{MRC}} = \frac{1}{2\Gamma(p)q^{\frac{L\phi^2}{2}}} \sum_{[j_i=0]_{i=1}^L}^{\infty} \prod_{l=1}^L \frac{\phi^2 m_l^{m_l}}{2S_0^{\phi^2} \Gamma(m_l)} \frac{K_l^{j_l} d_{l j_l}}{[\Gamma(j_l+1)]^2 (2\sigma_l^2 \gamma_0)^{\phi^2/2}} H_{2,1:2,2;2,2;\dots;2,2}^{0,1:2,1;2,1;\dots;2,1} \left[F(\gamma_0) \left| \begin{matrix} F_1 \\ F_2 \end{matrix} \right. \right]$$

where $F(\gamma_0) = \left\{ \frac{1}{2\sigma_i^2 S_0^2 \gamma_0 q} \right\}_{i=1}^L$, $F_1 = \left\{ (1 - p - \frac{L\phi^2}{2}; 1, \dots, 1) \right\}$, $F_2 = \left\{ (1 - \frac{\phi^2}{2}, 1), (1, 1) \right\}; \dots; \left\{ (1 - \frac{\phi^2}{2}, 1), (1, 1) \right\}$ and $F_2 = \left\{ (-\frac{L\phi^2}{2}; 1, \dots, 1) \right\}; \left\{ (-\frac{\phi^2}{2} + j_i + 1, 1), (0, 1) \right\}_{i=1}^L$. Similar to the outage probability, we get the asymptotic expression in (13) and the diversity order as $\sum_{l=1}^L \min\{j_l + 1, \phi^2/2\}$.

3) *Ergodic Capacity*: Substituting $f_\gamma(\gamma)$ in (16) and applying the definition of multivariate Fox's H-function [44]:

$$\bar{\eta}^{\text{MRC}} = \sum_{[j_i=0]_{i=1}^L}^{\infty} \prod_{l=1}^L \left(\frac{\gamma^2 m_l^{m_l}}{2A_0^{\phi^2} \Gamma(m_l)} \frac{K_l^{j_l} d_{l j_l}}{[\Gamma(j_l+1)]^2 (2\sigma_l^2 \gamma_0)^{\phi^2/2}} \right) \left(\frac{1}{2\pi i} \right)^L \int_{\mathcal{L}} \frac{1}{\Gamma\left(\frac{L\phi^2}{2} + \sum_{l=1}^L \zeta_l\right)} \left\{ \prod_{l=1}^L \frac{\Gamma\left(-\frac{\gamma^2}{2} + j_l + 1 - \zeta_l\right) \Gamma(-\zeta_l) \Gamma\left(\frac{\gamma^2}{2} + \zeta_l\right)}{\Gamma(1 - \zeta_l)} \left(\frac{1}{2\sigma_l^2 S_0^2 \gamma_0} \right)^{\zeta_l} d\zeta \right\} \frac{1}{\ln(2)} \int_0^\infty \ln(1+z) z^{-1 + \sum_{l=1}^L \left(\frac{\gamma^2}{2} + \zeta_l\right)} dz \quad (21)$$

We use the Mellin's inverse transform $\ln(1+z) = \frac{1}{2\pi i} \int_{L+1}^{\infty} \frac{\Gamma(1+\zeta_{L+1}) \Gamma(-\zeta_{L+1}) \Gamma(-\zeta_{L+1})}{\Gamma(1-\zeta_{L+1})} z^{-\zeta_{L+1}} d\zeta_{L+1}$ to represent the inner integral in (21) as

$$I_2 = \frac{1}{\ln(2) 2\pi i} \int_{L+1}^{\infty} \frac{\Gamma(1+\zeta_{L+1}) \Gamma(-\zeta_{L+1}) \Gamma(-\zeta_{L+1})}{\Gamma(1-\zeta_{L+1})} d\zeta_{L+1} \times \int_0^\infty z^{-1 + \sum_{l=1}^L \left(\frac{\gamma^2}{2} + \zeta_l\right)} z^{-\zeta_{L+1}} dz \quad (22)$$

Since the inner integral in (22) is not convergent, we use final value theorem $\lim_{t \rightarrow \infty} \int_0^t f(z) dz = \lim_{s \rightarrow 0} F(s) = F(\epsilon)$ with Laplace transform of integrand in (22) to get

$$I_{21} = \int_0^\infty z^{-1 + \sum_{l=1}^L \left(\frac{\gamma^2}{2} + \zeta_l\right)} z^{-\zeta_{L+1}} dz = \Gamma\left(\frac{L\phi^2}{2} + \sum_{l=1}^{L+1} \zeta_l - \zeta_{L+1}\right) \left(\frac{1}{\epsilon}\right)^{\frac{L\phi^2}{2} + \sum_{l=1}^{L+1} \zeta_l - \zeta_{L+1}} \quad (23)$$

Using (22) and (23) in (21), and applying the definition of

multivariate Fox's H-function, we get

$$\bar{\eta}^{\text{MRC}} = 1.4427 \sum_{[j_i=0]_{i=1}^L}^{\infty} \prod_{l=1}^L \frac{\phi^2 m_l^{m_l}}{2A_0^{\phi^2} \Gamma(m_l)} \frac{K_l^{j_l} d_{l j_l}}{[\Gamma(j_l+1)]^2 (2\sigma_l^2 \gamma_0 \epsilon)^{\phi^2/2}} H_{1,1:1,2;2,2;2,2;\dots;2,2;2,2}^{0,1:2,1;2,1;\dots;2,1;2,1} \left[\begin{matrix} G(\gamma_0) \\ \epsilon \end{matrix} \left| \begin{matrix} G_1 \\ G_2 \end{matrix} \right. \right] \quad (24)$$

where $G(\gamma_0) = \left\{ \frac{\gamma}{2\sigma_i^2 S_0^2 \gamma_0 \epsilon} \right\}_{i=1}^L$, $G_1 = \left\{ (1 - \frac{L\phi^2}{2}; 1, \dots, 1, -1) \right\}; \left\{ (1 - \frac{\phi^2}{2}, 1), (1, 1) \right\}; \dots; \left\{ (1 - \frac{\phi^2}{2}, 1), (1, 1) \right\}; \left\{ (0, 1), (1, 1) \right\}$ and $G_2 = \left\{ (1 - \frac{L\phi^2}{2}; 1, \dots, 1, 0) \right\}; \left\{ (-\frac{\phi^2}{2} + j_1 + 1, 1), (0, 1) \right\}_{i=1}^L; \left\{ (0, 1), (1, 1) \right\}$ where $\epsilon \rightarrow 0$.

V. SIMULATION AND NUMERICAL RESULTS

In this section, we demonstrate the performance of the considered single-antenna and MRC receivers for THz transmissions and validate the derived analytical expressions with Monte Carlo simulations. We consider the THz channel with a distance of 50m, carrier frequency 275 GHz, and antenna gains of 50 dBi. To compute the path loss for the THz link, we consider the relative humidity, atmospheric pressure, and temperature as 50%, 101325 Pa, and 296 K, respectively. We use [37] to compute the parameters ϕ and S_0 of pointing errors by varying the beamwidth and the jitter variance 10cm antenna aperture radius. The AWGN noise power is considered to be -94.2 dBm.

Fig. 1(a) demonstrates the impact of receiver antennas L , pointing errors parameter ϕ , and FTR fading m on the outage performance of the considered THz system with $S_0 = 0.054$, $\gamma_{\text{th}} = 4\text{dB}$, $K = 10$, and $\Delta = 0.5$. It can be seen that improvement in the performance is significant with spatial diversity when the number of receiver antennas is increased from $L = 1$ to $L = 4$. The figure also confirms that the outage probability improves when the fading severity parameter m increases, as expected. The slope of plots clearly demonstrate the dependence of diversity order on the system parameters. It can be seen that there is a distinguishable difference in the slopes for $\phi = 1$ and $\phi = 2.5$ but there is a minimal change in the slope with $\phi = 2.5$ and $\phi = 6$. As such, the

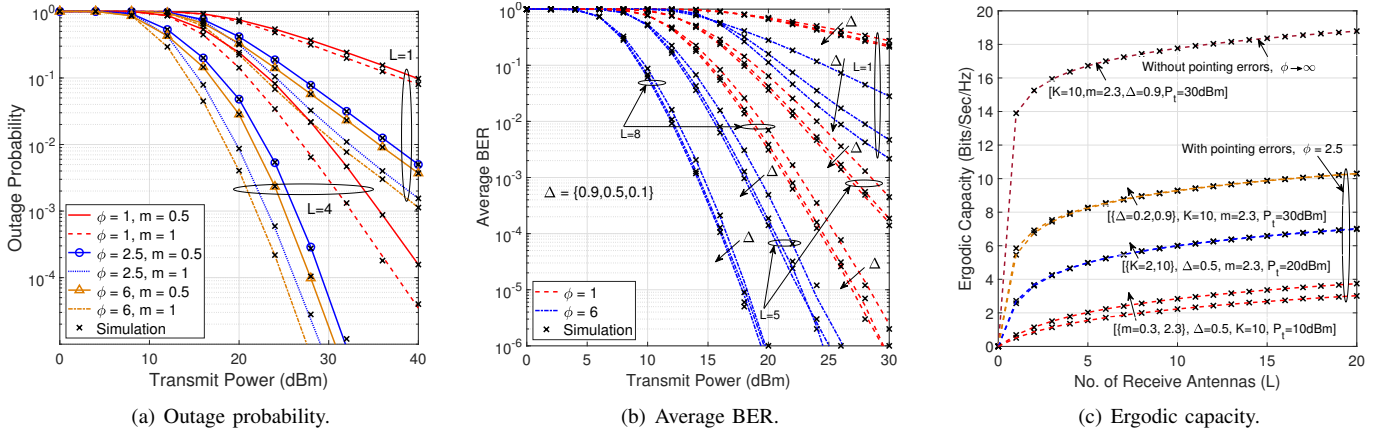


Fig. 1. Performance of THz wireless transmissions over FTR fading with pointing errors.

diversity order increases linearly with L , is independent of the parameter m , depends on ϕ when $\phi^2/2 < \min j_l + 1$ but becomes independent otherwise. Thus, the impact of pointing errors can be mitigated using a sufficiently higher beam-width for THz transmissions.

We demonstrate the average BER performance by varying the parameters Δ and ϕ with $K = 2$, and $m = 2$. The figure shows that highly dissimilar specular components of FTR fading depicted through Δ provides an improved average BER performance. Similar to the outage probability, we can observe that the average BER improves with an increase in the number of receiver antennas L and the diversity order is independent of Δ and becomes independent of pointing errors with a sufficiently higher value of ϕ .

Finally, Fig. 1(c) illustrates the relationship between the ergodic capacity and the number of receiver antennas with interdependence of the various channel and system parameters. The figure shows the logarithmic scaling of the ergodic capacity with the number of receiver antennas L . It can be observed that ergodic capacity is nearly independent of the parameters K and Δ , but increases with an increase in the parameters m . The figure also shows that pointing errors significantly degrade the THz performance. However, an increase in the MRC antennas reduces the gap in performance by harnessing the spatial as compared to the single-antenna system.

VI. CONCLUSIONS

In this paper, we analyzed the performance of THz wireless transmissions under the combined effects of path loss, generalized FTR fading, and Rayleigh distributed pointing errors. We provided statistical results on the single-antenna and multi-antenna receivers by deriving PDF and CDF of the resultant SNR. We analyzed the performance of the considered system by deriving closed-form expressions for the outage probability, average BER, and ergodic capacity. Using asymptotic analysis on the outage probability and average BER, we derived the diversity order of the system, which provides a design criterion of using sufficiently higher beam-width to mitigate the impact of pointing errors by circumventing the multi-path fading. We validated our derived analytical expressions with Monte-Carlo simulations to show that the impact of the number of receiver antennas L , pointing errors ϕ , and fading severity

parameter m is higher on the THz wireless system compared with other parameters. Incorporating hardware impairment in the performance analysis may be a possible extension of the proposed work.

APPENDIX A

Using the definition of the MGF function, we apply inverse Laplace transform to find the PDF of $\gamma = \sum_{i=1}^L \gamma_i$ as $f_\gamma(\gamma) = \mathcal{L}^{-1}M_\gamma(s)$, where $M_\gamma(s) = \prod_{i=1}^L M_{\gamma_i}(s)$ and $M_{\gamma_i}(s)$ is the MGF of the i -th random variable γ_i . Converting the incomplete Gamma function in (5) to Meijer's G and applying the Meijer's G identity of definite integration, we get

$$M_\gamma(s) = \prod_{l=1}^L \frac{\phi^2 m_l m_l}{2S_0^{\phi^2} \Gamma(m_l)} \sum_{[j_i=0]_{i=1}^L}^{\infty} \frac{K_l^{j_l} d_l j_l s^{-\frac{\phi^2}{2}}}{[\Gamma(j_l+1)]^2 (2\sigma_l^2 \gamma_0)^{\phi^2/2}} G_{2,2}^{2,1} \left(\frac{1}{2\sigma_l^2 S_0^2 \gamma_0 s} \left| \begin{matrix} -\frac{\phi^2}{2} + 1, 1 \\ -\frac{\phi^2}{2} + j_l + 1, 0 \end{matrix} \right. \right) \quad (25)$$

Applying the definition of Meijer's G function [42] and interchanging the sum and product, we get

$$M_\gamma(s) = \sum_{[j_i=0]_{i=1}^L}^{\infty} \prod_{l=1}^L \left(\frac{\phi^2 m_l m_l}{2S_0^{\phi^2} \Gamma(m_l)} \frac{K_l^{j_l} d_l j_l s^{-\frac{\phi^2}{2}}}{[\Gamma(j_l+1)]^2 (2\sigma_l^2 \gamma_0)^{\phi^2/2}} \right) \frac{1}{2\pi i} \int_{L_l} \frac{\Gamma(-\frac{\phi^2}{2} + j_l + 1 - \zeta_l) \Gamma(-\zeta_l) \Gamma(\frac{\phi^2}{2} + \zeta_l)}{\Gamma(1 - \zeta_l)} \left(\frac{1}{2\sigma_l^2 S_0^2 \gamma_0 s} \right)^{\zeta_l} d\zeta_l \quad (26)$$

Thus, using $f_\gamma(z) = \frac{1}{2\pi i} \int_L e^{sz} M_\gamma(s) ds$, interchanging the integral, and rearranging the terms, we get

$$f_\gamma(z) = \sum_{[j_i=0]_{i=1}^L}^{\infty} \prod_{l=1}^L \left(\frac{\phi^2 m_l m_l}{2S_0^{\phi^2} \Gamma(m_l)} \frac{K_l^{j_l} d_l j_l}{[\Gamma(j_l+1)]^2 (2\sigma_l^2 \gamma_0)^{\phi^2/2}} \right) \prod_{l=1}^L \frac{1}{2\pi i} \int_{L_l} \frac{\Gamma(-\frac{\phi^2}{2} + j_l + 1 - \zeta_l) \Gamma(-\zeta_l) \Gamma(\frac{\phi^2}{2} + \zeta_l)}{\Gamma(1 - \zeta_l)} \left(\frac{1}{2\sigma_l^2 S_0^2 \gamma_0} \right)^{\zeta_l} \frac{1}{2\pi i} \int_L e^{sz} s^{-\sum_{l=1}^L (\frac{\phi^2}{2} + \zeta_l)} ds d\zeta_l \quad (27)$$

We substitute $sz = -b$, and apply the identity [41] (eq.

8.315.1) to solve the inner integral in (27):

$$I = \frac{1}{2\pi i} \int_L e^{sz} s^{-\sum_{l=1}^L (\frac{\phi^2}{2} + \zeta_l)} ds = \frac{z^{-1 + \sum_{l=1}^L (\frac{\phi^2}{2} + \zeta_l)}}{\Gamma\left(\sum_{l=1}^L \left(\frac{\phi^2}{2} + \zeta_l\right)\right)} \quad (28)$$

We substitute (28) in (27) and apply the definition of multivariate Fox's H function [44] to get (10). Finally, we use $F_\gamma(z) = \mathcal{L}^{-1} \prod_{i=1}^N \frac{M_{\gamma_i}(s)}{s}$ and apply the similar steps used in the derivation of PDF to get the CDF in (11), which concludes the proof of Theorem 1.

REFERENCES

- [1] S. Koenig *et al.*, "Wireless sub-THz communication system with high data rate," *Nature Photon.*, vol. 7, p. 977–981, 2013.
- [2] C. Wang *et al.*, "0.34-THz wireless link based on high-order modulation for future wireless local area network applications," *IEEE Trans. THz Sci. Technol.*, vol. 4, no. 1, pp. 75–85, 2014.
- [3] H. Elayan *et al.*, "Terahertz band: The last piece of RF spectrum puzzle for communication systems," *IEEE Open J. of the Commun. Soc.*, vol. 1, pp. 1–32, 2020.
- [4] J. Kokkonen *et al.*, "Simplified molecular absorption loss model for 275–400 GHz wireless link," in *12th Eur. Conf. on Antennas Propag. (EuCAP)*, Apr. 2018, pp. 1–5.
- [5] —, "Impact of beam misalignment on THz wireless systems," *Nano Commun. Netw.*, vol. 24, p. 100302, 2020.
- [6] A. A. Boulogeorgos and A. Alexiou, "Analytical performance assessment of THz wireless systems," *IEEE Access*, vol. 7, pp. 11 436–11 453, 2019.
- [7] S. Liu *et al.*, "THz channel modeling: Consolidating the road to THz communications," *China Communications*, vol. 18, no. 5, pp. 33–49, 2021.
- [8] Q. Xia and J. M. Jornet, "Cross-layer analysis of optimal relaying strategies for Terahertz-band communication networks," in *2017 IEEE 13th Int. Conf. on Wireless and Mobile Comput., Netw. and Commun. (WiMob)*, 2017, pp. 1–8.
- [9] G. Stratidakis *et al.*, "Relay-based blockage and antenna misalignment mitigation in THz wireless communications," in *2020 2nd 6G Wireless Summit (6G SUMMIT)*, 2020, pp. 1–4.
- [10] A.-A. Boulogeorgos and A. Alexiou, "Outage probability analysis of THz relaying systems," in *2020 IEEE 31st Annu. Int. Symp. on Personal, Indoor and Mobile Radio Commun.*, 2020, pp. 1–7.
- [11] C. Huang *et al.*, "Multi-hop RIS-empowered Terahertz communications: A DRL-based hybrid beamforming design," *IEEE J. Sel. Areas Commun.*, vol. 39, no. 6, pp. 1663–1677, 2021.
- [12] A. A. Boulogeorgos and A. Alexiou, "Error analysis of mixed THz-RF wireless systems," *IEEE Commun. Lett.*, vol. 24, no. 2, pp. 277–281, 2020.
- [13] P. Bhardwaj and S. M. Zafaruddin, "Performance analysis of dual-hop relaying for THz-RF wireless link over asymmetrical $\alpha - \mu$ fading," *IEEE Trans. on Veh. Technol.*, pp. 1–1, 2021.
- [14] Z. Rong *et al.*, "Relay-assisted nanoscale communication in the THz band," *Micro Nano Lett.*, vol. 12, no. 6, pp. 373–376, 2017.
- [15] Q. H. Abbasi *et al.*, "Cooperative In-Vivo nano-network communication at Terahertz frequencies," *IEEE Access*, vol. 5, pp. 8642–8647, 2017.
- [16] T. Mir *et al.*, "Hybrid precoding design for two-way relay-assisted Terahertz massive MIMO systems," *IEEE Access*, vol. 8, pp. 222 660–222 671, 2020.
- [17] A. R. Ekti *et al.*, "Statistical modeling of propagation channels for terahertz band," in *2017 IEEE Conference on Standards for Communications and Networking (CSCN)*, 2017, pp. 275–280.
- [18] T. Kursat *et al.*, "Modeling and analysis of short distance sub-terahertz communication channel via mixture of gamma distribution," *IEEE Transactions on Vehicular Technology*, vol. 70, no. 4, pp. 2945–2954, 2021.
- [19] E. N. Papasotiriou *et al.*, "A new look to THz wireless links: Fading modeling and capacity assessment," in *2021 IEEE 32nd Annu. Int. Symp. on Personal, Indoor and Mobile Radio Commun.*, 2021, pp. 1–6.
- [20] H. Du, J. Zhang, K. Guan, B. Ai, and T. Kürner, "Reconfigurable intelligent surface aided terahertz communications under misalignment and hardware impairments," *arXiv:2012.00267*, 2020.
- [21] K. Guan *et al.*, "Measurement, simulation, and characterization of train-to-infrastructure inside-station channel at the terahertz band," *IEEE Transactions on Terahertz Science and Technology*, vol. 9, no. 3, pp. 291–306, 2019.
- [22] J. M. Romero-Jerez *et al.*, "The fluctuating two-ray fading model: Statistical characterization and performance analysis," *IEEE Transactions on Wireless Communications*, vol. 16, no. 7, pp. 4420–4432, 2017.
- [23] J. Zhang, W. Zeng, X. Li, Q. Sun, and K. P. Peppas, "New results on the fluctuating two-ray model with arbitrary fading parameters and its applications," *IEEE Transactions on Vehicular Technology*, vol. 67, no. 3, pp. 2766–2770, 2018.
- [24] H. Zhao *et al.*, "Different power adaption methods on fluctuating two-ray fading channels," *IEEE Wireless Communications Letters*, vol. 8, no. 2, pp. 592–595, 2019.
- [25] W. Zeng, J. Zhang, S. Chen, K. P. Peppas, and B. Ai, "Physical layer security over fluctuating two-ray fading channels," *IEEE Transactions on Vehicular Technology*, vol. 67, no. 9, pp. 8949–8953, 2018.
- [26] Y. Zhang *et al.*, "On the performance of dual-hop systems over mixed FSO/mmWave fading channels," *IEEE Open J. of the Commun. Soc.*, vol. 1, pp. 477–489, 2020.
- [27] O. S. Badarneh and D. B. da Costa, "Cascaded fluctuating two-ray fading channels," *IEEE Communications Letters*, vol. 23, no. 9, pp. 1497–1500, 2019.
- [28] H. Hashemi *et al.*, "Analysis of equal gain combining over fluctuating two-ray channels with applications to millimeter-wave communications," *IEEE Transactions on Vehicular Technology*, vol. 69, no. 2, pp. 1751–1765, 2020.
- [29] H. Al-Hmood and H. S. Al-Raweshidy, "Performance analysis of mmwave communications with selection combining over fluctuating two ray fading model," *IEEE Communications Letters*, pp. 1–1, 2021.
- [30] J. Zheng *et al.*, "Sum of squared fluctuating two-ray random variables with wireless applications," *IEEE Transactions on Vehicular Technology*, vol. 68, no. 8, pp. 8173–8177, 2019.
- [31] M. Olyaei *et al.*, "Performance of maximum ratio combining of fluctuating two-ray FTR mmWave channels for 5G and beyond communications," *Transactions on Emerging Telecommunications Technologies*, vol. 30, no. 10, 2019.
- [32] H. Hashemi *et al.*, "Amplify-and-forward relaying with maximal ratio combining over fluctuating two-ray channel: Non-asymptotic and asymptotic performance analysis," *IEEE Transactions on Communications*, vol. 68, no. 12, pp. 7446–7459, 2020.
- [33] J. Zhang *et al.*, "Performance analysis of 5G mobile relay systems for high-speed trains," *IEEE Journal on Selected Areas in Communications*, vol. 38, no. 12, pp. 2760–2772, 2020.
- [34] H. R. Alhennawi *et al.*, "Closed-form exact and asymptotic expressions for the symbol error rate and capacity of the H-function fading channel," *IEEE Trans. Veh. Technol.*, vol. 65, no. 4, pp. 1957–1974, 2016.
- [35] P. Bhardwaj and S. M. Zafaruddin, "Performance of dual-hop relaying for THz-RF wireless link," in *2021 IEEE 93rd Veh. Technol. Conf. (VTC2021-Spring)*, 2021, pp. 1–5.
- [36] A. A. Boulogeorgos *et al.*, "Performance evaluation of THz wireless systems operating in 275–400 GHz band," in *2018 IEEE 87th Vehicular Technology Conference (VTC Spring)*, 2018, pp. 1–5.
- [37] A. A. Farid and S. Hranilovic, "Outage capacity optimization for free-space optical links with pointing errors," *J. Lightw. Technol.*, vol. 25, no. 7, pp. 1702–1710, 2007.
- [38] M. López-Benítez and J. Zhang, "Comments and corrections to "new results on the fluctuating two-ray model with arbitrary fading parameters and its applications"," *IEEE Transactions on Vehicular Technology*, vol. 70, no. 2, pp. 1938–1940, 2021.
- [39] A. Papoulis and S. Pillai, *Probability, Random Variables, and Stochastic Processes*. McGraw Hill, Boston, Fourth Edition, 2002.
- [40] I. S. Ansari *et al.*, "A new formula for the BER of binary modulations with dual-branch selection over generalized-k composite fading channels," *IEEE Transactions on Communications*, vol. 59, no. 10, pp. 2654–2658, 2011.
- [41] I. S. Gradshteyn and I. M. Ryzhik, *Table of Integrals, Series, and Products*. Academic press, San Diego, CA, 6th edition, 2000.
- [42] *The Wolfram function Site*, Accessed: July 28, 2021. Available: <https://functions.wolfram.com/HypergeometricFunctions/MeijerG/>.
- [43] Y. Abo Rahama *et al.*, "On the sum of independent Fox's H -function variates with applications," *IEEE Transactions on Vehicular Technology*, vol. 67, no. 8, pp. 6752–6760, 2018.
- [44] A. A. Kilbas, *H-Transforms: Theory and Applications*. CRC Press, 2004, vol. First edition.